Non-linear standing wave effects on the weather side of a wall with a narrow gap

B. Molin, O. Kimmoun, F. Remy

École Centrale Marseille, 13 451 Marseille cedex 20 (bmolin@ec-marseille.fr)

Introduction

For the past 4 or 5 years we have been studying runup phenomena along reflective structures such as barges in beam seas, GBS platforms or vertical plates. We have demonstrated, through dedicated experimental, theoretical and numerical modeling, that these phenomena result from third-order interactions between the incoming and reflected waves on the weather side of the structure: the reflected waves act as a shoal to the incoming waves, slowing them down and inducing focussing effects.

In Molin *et al.* (2005) we consider a vertical plate with an equivalent length of 2.4 m[1] in beam regular waves of wavelengths ranging from 1.2 to 3 m. Strong runups are obtained located at mid-plate. They turn out to be well predicted by a simplified model accounting heuristically for the tertiary interactions between incoming and reflected waves. Good agreement is also obtained with a numerical wave-tank based on so-called extended Boussinesq equations (Jamois *et al.*, 2006). In an other series of experiments a longer plate (2×3 m) is subjected to regular waves of wavelengths in the range 0.6 to 2 m. Again good agreement is obtained between measured and calculated free surface elevations along the plate, with the two numerical models reproducing the notable feature that a standing wave pattern takes place along the plate, with a node some distance from the plate edge (figure 1 taken from Molin *et al.* 2006).

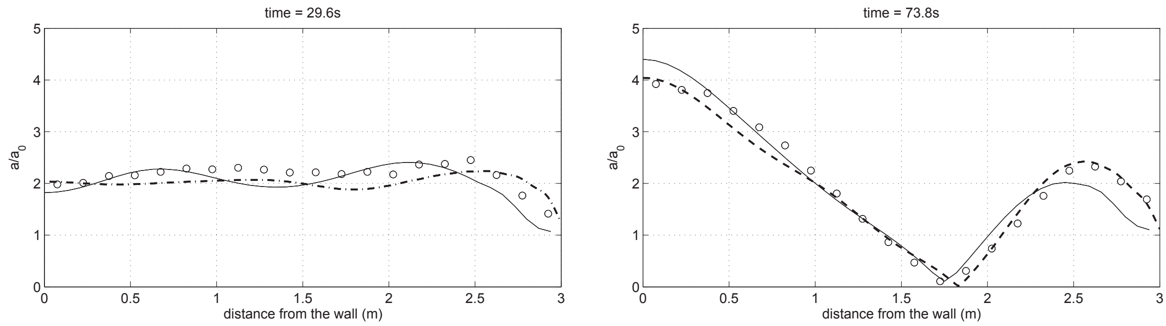

Fig. 1 – *Wave period: 0.95 s. Steepness $H/L = 4$ %. Profiles along the plate of the measured (circles) and calculated normalized wave amplitudes shortly after arrival of the wave front (left) and after 65 wave cycles (right). The thick dash-dotted and dashed lines show the frequency domain calculations, linear and nonlinear; the thinner line shows the time domain calculations.*

As the wavelength gets shorter as compared to the plate length the effective interaction area increases in size and transients last longer and longer. As a matter of fact it is not obvious that steady states can always be reached and the nonlinear frequency domain model usually does not converge when the wave steepness exceeds some value: the larger the plate length over wavelength ratio, the smaller the limiting steepness. The case of a semi-infinite wall is quite puzzling.

In this paper we consider the "anti-plate" problem, that is an infinite wall with a gap. One of our incentives is the conjecture that tertiary interactions between the incoming and reflected waves might lead to defocussing effects, that is much less wave energy traveling trough the opening than predicted by linear theory. This would have some relevance for wave energy converters set on a reflective coastline, such as some OWC converters. The linear case is well-known, see for instance Mei (1983) for the case of a narrow gap, or Morse & Feshbach (1953) who offer an analytical solution.

A major difference with the case of an isolated plate is that, the reflected wave-field being as strong as the incoming wave-field, its modification under tertiary interaction with the incoming wave-field cannot be ignored. Therefore we extend the heuristic model described in Molin *et al.* (2005) to accounting for both modifications, with the incoming and reflected complex wave amplitudes obeying two coupled parabolic equations, which are solved successively through iterations. Preliminary results are given.

1. A 1.2 m long plate stuck against the wall.

Linear case

We assume infinite waterdepth. The incoming waves are regular with amplitude A_0 and frequency ω and propagate along the x direction. The wall is located in $x = 0$, $|y| \geq a$, with $2a$ the width of the gap. On the weather side of the wall the velocity potential is expressed as

$$\varphi = \frac{-2\,\mathrm{i}\,A_0\,g}{\omega}\,\mathrm{e}^{kz}\,\cos kx - \frac{\mathrm{i}\,A_0\,g}{\omega}\,\mathrm{e}^{kz}\int_{-a}^{a}\frac{\sigma(Y)}{\sqrt{a^2-Y^2}}\,H_0(k\sqrt{x^2+(y-Y)^2})\,\mathrm{d}Y \tag{1}$$

and on the lee side

$$\varphi = \frac{\mathrm{i}\,A_0\,g}{\omega}\,\mathrm{e}^{kz}\int_{-a}^{a}\frac{\sigma(Y)}{\sqrt{a^2-Y^2}}\,H_0(k\sqrt{x^2+(y-Y)^2})\,\mathrm{d}Y \tag{2}$$

Here $\Phi(x,y,z,t) = \Re\left\{\varphi(x,y,z)\,\mathrm{e}^{-\mathrm{i}\,\omega t}\right\}$ and H_0 is the Hankel function of zero order. The chosen form of the source distribution is related to the expected singularity at the gap edges.

Equations (1) and (2) ensure that $\partial\varphi/\partial x$ is continuous across the gap and nil at the wall. Matching of the potentials yields the integral equation

$$\int_{-a}^{a}\frac{\sigma(Y)}{\sqrt{a^2-Y^2}}\,H_0(k\,|y-Y|)\,\mathrm{d}Y = -1 \tag{3}$$

or

$$\int_0^{\pi/2}\sigma(\theta)\,\left\{H_0\left(ka\,|\sin\theta-\sin\phi|\right)+H_0\left(ka\,|\sin\theta+\sin\phi|\right)\right\}\,\mathrm{d}\theta = -1 \qquad \forall\,\phi\in[0\;\pi/2]. \tag{4}$$

Equation (4) is solved numerically by collocation.

Accounting for tertiary interactions

We express the velocity potentials of the incoming and reflected waves, on the weather side, under the forms

$$\varphi_I = \frac{-\mathrm{i}\,A_I(\epsilon^2 x,\epsilon y)\,g}{\omega}\,\mathrm{e}^{\mathrm{i}\,k(1+\epsilon^2)\,x}\,\mathrm{e}^{[k+\epsilon^2\,k_I^{(2)}]\,z} \tag{5}$$

$$\varphi_R = \frac{-\mathrm{i}\,A_R(\epsilon^2 x,\epsilon y)\,g}{\omega}\,\mathrm{e}^{-\mathrm{i}\,k(1+\epsilon^2)\,x}\,\mathrm{e}^{[k+\epsilon^2\,k_R^{(2)}]\,z} + \varphi_{\mathrm{gap}} \tag{6}$$

Here A_I and A_R are complex amplitudes, $\epsilon \equiv kA_0$ and φ_{gap} is the velocity potential of the wave system radiated from the gap.

Following Molin *et al.* (2005) we infer that A_I and A_R obey the coupled parabolic equations

$$2\mathrm{i}\;k\,A_{Ix} + A_{Iyy} + 2k^4\,A_I\,\left[2\widetilde{A}_R\,\widetilde{A}_R^* - A_I\,A_I^* - A_0^2\right] = 0 \tag{7}$$

$$-2\mathrm{i}\;k\,A_{Rx} + A_{Ryy} + 2k^4\,A_R\,\left[2A_I\,A_I^* - \widetilde{A}_R\,\widetilde{A}_R^* - A_0^2\right] = 0 \tag{8}$$

where $\widetilde{A}_R$ is the reflected wave amplitude A_R plus the local (complex) amplitude of the wave system radiated from the gap, which has the main effect of modulating the wave system that would be reflected from a wall with no gap.

To solve equations (7) and (8) we bound the fluid domain in x and y, introducing a wall in $y = b$ (alike in a wave-tank), and we expand A_I and A_R as

$$A_I = A_0\left(1+\sum_{n=0}^{N}a_n(x)\,\cos\lambda_n y\right) \qquad A_R = A_0\left(1+\sum_{n=0}^{N}b_n(x)\,\cos\lambda_n y\right) \tag{9}$$

with $\lambda_n = n\,\pi/b$. We assume that the incoming waves are generated in $x = -l$, meaning $a_n(-l) = 0$. The no-flow condition at the wall gives $b_n(0) = a_n(0)$, while the radiated wave system from the gap is obtained by solving the integral equation

$$\int_0^{\pi/2}\sigma(\theta)\,\left\{H_0\left(ka\,|\sin\theta-\sin\phi|\right)+H_0\left(ka\,|\sin\theta+\sin\phi|\right)\right\}\,\mathrm{d}\theta = -1-\sum_{n=0}^{N}a_n(0)\,\cos(\lambda_n a\,\sin\phi). \tag{10}$$

The coefficients a_n and b_n are updated through iterations (with relaxation) where the parabolic and integral equations (7), (10) and (8) are solved successively (equation (7) from $x = -l$ to the wall, equation (8) from the wall back to $x = -l$).

As an illustration we consider a gap length $2a$ equal to a wavelength, a domain width $2b$ of 20 wavelengths and an interaction length l of 10 wavelengths. Obtained wave patterns (normalized by the amplitude A_0) at wave steepnesses $H/L = kA_0/\pi$ of 1 and 3 % are shown in figures 2 and 3 (only half the domain $y > 0$ is shown).

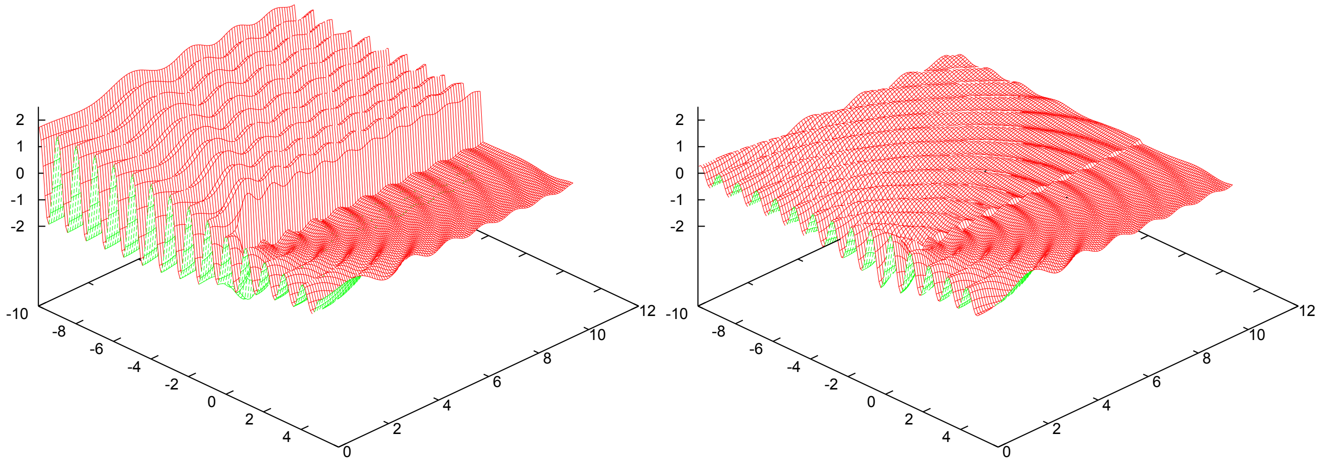

FIG. 2 – *Wave steepness $H/L = 1$ %. Gap width $ka = \pi$. Real (left) and imaginary (right) parts.*

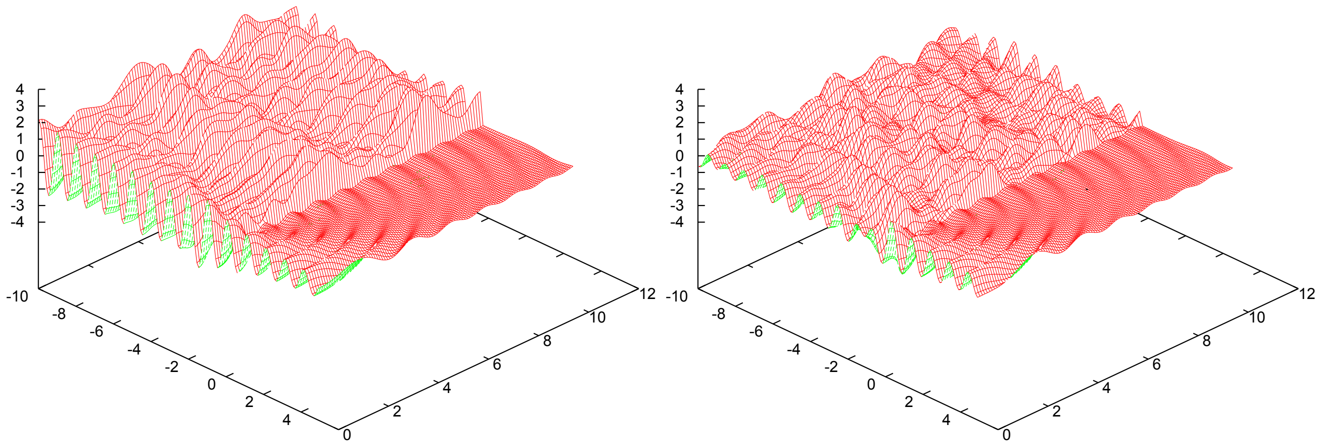

FIG. 3 – *Wave steepness $H/L = 3$ %. Gap width $ka = \pi$. Real (left) and imaginary (right) parts.*

At the lower steepness of 1 % the profiles are quasi-identical with the linear solution. However at the larger one a chaotic pattern is obtained with local elevations nearly 4 times as high as the incoming wave amplitude A_0. A very small gap is sufficient to produce these effects as figure 4 shows, for a gap equal to one eigth of the wavelength.

The profiles shown in figures 3 and 4 are obtained after over 100 iterations. They are numerically converged in the vicinity of the gap, however they keep on evolving by the opposite wall. Moreover they are very sensitive to changes in the size of the numerical domain, more particularly to the interaction length l. Figure 5 shows, for the first gap width, the RAOs of the free surface elevation along the gap and wall, for steepnesses H/L of 2, 2.5 and 3 %. Disappointingly the values at the gap do not decrease when the steepness increases. (The reverse is obtained with the numerical model of Molin *et al.* (2005) where modifications of the reflected wave system are not accounted for.)

All these results raise many questions:

– our parabolic equations are similar to the equations (3.3a) of Okamura (1984) who studies the stability of weakly nonlinear standing waves, with the difference that ours have no time dependent term (since we look for a steady state solution) and no dispersive term in x. In Molin *et al.* (2005) it was argued that the latter term would be higher order in ϵ owing to the space dependence of the forcing term. In the present case the forcing term (the modulation of the reflected wave system by the radiated waves from the gap) can be very weak.

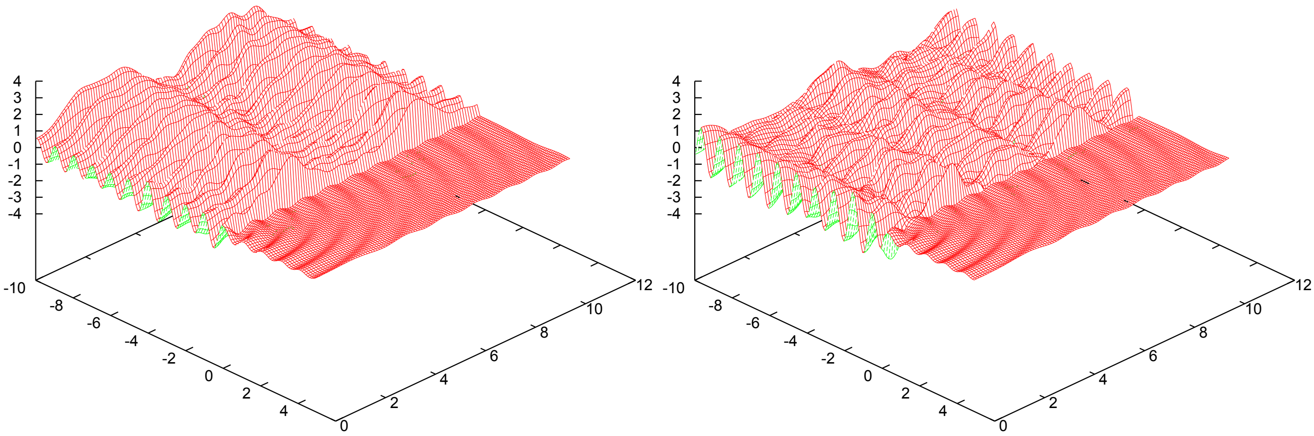

FIG. 4 – *Wave steepness $H/L = 3$ %. Gap width $ka = \pi/8$. Real (left) and imaginary (right) parts.*

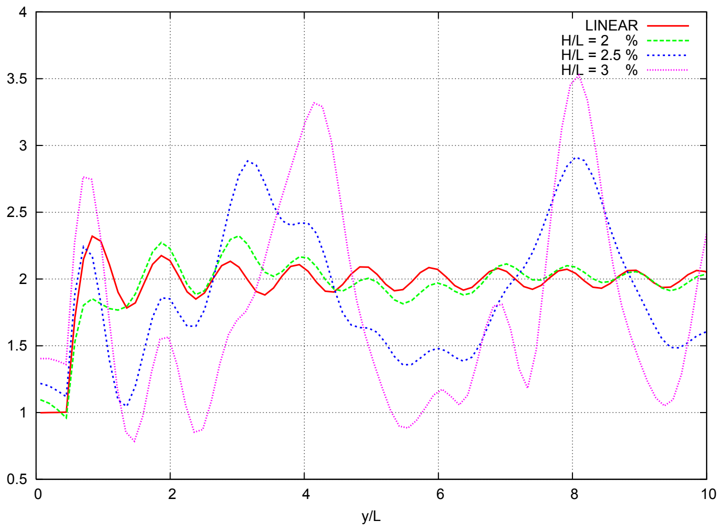

FIG. 5 – *Gap width $ka = \pi$. RAOs of the free surface elevation along the gap and wall for different wave steepnesses.*

– the way we introduce the radiated wave field in our parabolic equations (through $\widetilde{A}_R$) is based more on intuition than on sound reasoning.

– doubts can be raised on the meaningfulness of performing model tests on reflective coastal structures, in confined tanks.

Obviously it would be desirable to make comparisons with results from a fully non-linear numerical model such as Jamois'. So far Jamois' model has failed to yield satisfactory results on this new problem. Hopefully some will be available in time for the workshop.

References

JAMOIS E., D.R. FUHRMAN, H.B. BINGHAM & B. MOLIN 2006 A numerical study of nonlinear wave run-up on a vertical plate, *Coastal Engineering*, **53**, 929–945.

MEI C.C. 1983 *The applied dynamics of ocean surface waves*, Wiley-Interscience.

MOLIN B., O. KIMMOUN, F. REMY & E. JAMOIS 2006 Non-linear wave interaction with a long vertical breakwater, *Proc. 7th Int. Conf. Hydrodynamics*, Ischia.

MOLIN B., F. REMY, O. KIMMOUN & E. JAMOIS 2005 The role of tertiary wave interactions in wave-body problems, *J. Fluid Mech.*, **528**, 323–354.

MORSE P.M. & H. FESHBACH 1953 *Methods of theoretical physics*, New-York: McGraw-Hill.

OKAMURA M. 1984 Instabilities of weakly nonlinear standing gravity waves, *J. Phys. Soc. Japan*, **53**, 3788–3796.